

Diagnostic Accuracy of Stress Perfusion CMR in Comparison With Quantitative Coronary Angiography

Fully Quantitative, Semiquantitative, and Qualitative Assessment

Federico E. Mordini, MD,*† Tariq Haddad, MD,* Li-Yueh Hsu, DSc,* Peter Kellman, PhD,* Tracy B. Lowrey, RN,* Anthony H. Aletras, PhD,*† W. Patricia Bandettini, MD,* Andrew E. Arai, MD*

Bethesda, Maryland; Washington, DC; and Lamia, Greece

OBJECTIVES This study's primary objective was to determine the sensitivity, specificity, and accuracy of fully quantitative stress perfusion cardiac magnetic resonance (CMR) versus a reference standard of quantitative coronary angiography. We hypothesized that fully quantitative analysis of stress perfusion CMR would have high diagnostic accuracy for identifying significant coronary artery stenosis and exceed the accuracy of semiquantitative measures of perfusion and qualitative interpretation.

BACKGROUND Relatively few studies apply fully quantitative CMR perfusion measures to patients with coronary disease and comparisons to semiquantitative and qualitative methods are limited.

METHODS Dual bolus dipyridamole stress perfusion CMR exams were performed in 67 patients with clinical indications for assessment of myocardial ischemia. Stress perfusion images alone were analyzed with a fully quantitative perfusion (QP) method and 3 semiquantitative methods including contrast enhancement ratio, upslope index, and upslope integral. Comprehensive exams (cine imaging, stress/rest perfusion, late gadolinium enhancement) were analyzed qualitatively with 2 methods including the Duke algorithm and standard clinical interpretation. A 70% or greater stenosis by quantitative coronary angiography was considered abnormal.

RESULTS The optimum diagnostic threshold for QP determined by receiver-operating characteristic curve occurred when endocardial flow decreased to <50% of mean epicardial flow, which yielded a sensitivity of 87% and specificity of 93%. The area under the curve for QP was 92%, which was superior to semiquantitative methods: contrast enhancement ratio: 78%; upslope index: 82%; and upslope integral: 75% ($p = 0.011$, $p = 0.019$, $p = 0.004$ vs. QP, respectively). Area under the curve for QP was also superior to qualitative methods: Duke algorithm: 70%; and clinical interpretation: 78% ($p < 0.001$ and $p < 0.001$ vs. QP, respectively).

CONCLUSIONS Fully quantitative stress perfusion CMR has high diagnostic accuracy for detecting obstructive coronary artery disease. QP outperforms semiquantitative measures of perfusion and qualitative methods that incorporate a combination of cine, perfusion, and late gadolinium enhancement imaging. These findings suggest a potential clinical role for quantitative stress perfusion CMR. (J Am Coll Cardiol Img 2014;7:14–22) © 2014 by the American College of Cardiology Foundation

Cardiac magnetic resonance (CMR) has potential advantages in the assessment of myocardial perfusion. Diagnostically, CMR appears superior to single-photon emission computed tomography (SPECT) (1–3). Comparisons to positron emission tomography (PET) are favorable (4), and similar to PET, CMR can quantify perfusion in absolute terms (5–7). However, CMR has finer resolution, wider availability, and can evaluate function, perfusion, and viability in the same exam without ionizing radiation.

See page 23

Although semiquantitative CMR perfusion has been evaluated in the setting of coronary artery disease (CAD), semiquantitative techniques underestimate perfusion at high flow rates and have a potential diagnostic disadvantage when compared with fully quantitative perfusion, which increases linearly over a wide range of flow rates (8). However, fully quantitative studies in humans with CAD have been limited and lack adequate comparisons with semiquantitative and qualitative analyses (9–15).

Quantifying myocardial perfusion using a dual-bolus first-pass CMR method has been validated against microspheres in a canine model, and all major findings have been confirmed in normal human volunteers (8,16). To investigate the clinical utility of this technique, we applied the method to patients with known or suspected coronary disease.

Our primary objective was to determine the sensitivity, specificity, and accuracy of fully quantitative dual-bolus stress perfusion CMR versus a reference standard of quantitative coronary angiography (QCA). We hypothesized that fully quantitative analysis of stress perfusion CMR would have high diagnostic accuracy for identifying significant coronary artery stenosis. We also hypothesized that the diagnostic accuracy of the fully quantitative method would exceed that of semiquantitative and qualitative methods of interpretation. Finally, we sought to demonstrate that detailed stress perfusion analysis independently contains the diagnostic information necessary to detect the presence of significant coronary disease.

METHODS

Patients. This study was approved by the institutional review boards of the National Institutes of Health and Suburban Hospital (Bethesda, Maryland). All patients were referred for stress myocardial perfusion imaging with clinical indications. Sixty-seven subjects with coronary angiography performed within 90 days of the CMR were included on a consecutive basis. Subjects with recent percutaneous coronary intervention, history of coronary bypass surgery, contraindication to dipyridamole, or contraindication to CMR were excluded.

Image acquisition. Imaging was performed on a 1.5-T Siemens (Erlangen, Germany) or General Electric (Waukesha, Wisconsin) scanner using a 12-element or 4-element phased array coil, respectively. Gadolinium-diethylenetriaminepentaacetic acid (Magnevist, Bayer HealthCare Pharmaceuticals, Whippany, New Jersey) was administered with a mechanical injector (Medrad, Inc., Indianola, Pennsylvania). The exam proceeded in the following sequence: stress perfusion; cine rest function; rest perfusion; and late gadolinium enhancement imaging (LGE).

The vasodilator stress protocol used dipyridamole 0.56 mg/kg infused intravenously over 4 min. Perfusion imaging commenced 4 min after the dipyridamole infusion. Dual-bolus first-pass perfusion was performed using gadolinium doses of 0.005 mmol/kg followed by 0.1 mmol/kg (16). The 0.005 mmol/kg dose was diluted in saline to ensure equal volume and rates of injection for the 2 doses. Three short-axis images were acquired using a saturation recovery, hybrid echo-planar perfusion sequence for every heart beat for 50 to 60 cardiac cycles (17). Typical imaging parameters were as follows: slice thickness: 8 mm; field of view: 360 mm × 270 mm; repetition time: 6.6 to 7.5 ms; echo time: 1.48 to 1.6 ms; echo train length: 4; matrix: 128 × 80 to 128 × 96; flip angle: 20° to 25°; and saturation recovery time: 60 to 80 ms. Parallel imaging with rate 2 temporal sensitivity encoding was

ABBREVIATIONS AND ACRONYMS

AUC	= area under the curve
CAD	= coronary artery disease
CER	= contrast enhancement ratio
CMR	= cardiac magnetic resonance
INT	= upslope integral
LGE	= late gadolinium enhancement
PET	= positron emission tomography
QCA	= quantitative coronary angiography
QP	= fully quantitative perfusion
ROC	= receiver-operating characteristic
SI	= signal intensity
SLP	= myocardial to left ventricular upslope ratio
SPECT	= single-photon emission computed tomography

From the *Cardiovascular and Pulmonary Branch, National Heart, Lung, and Blood Institute, National Institutes of Health, Department of Health and Human Services, Bethesda, Maryland; †Department of Cardiology, Veterans Affairs Medical Center, Washington, DC; and ‡Department of Biomedical Informatics, University of Central Greece, Lamia, Greece. This study was funded by the Division of Intramural Research, National Heart, Lung, and Blood Institute, National Institutes of Health. Dr. Arai receives research support from Siemens Medical Imaging (United States Government Cooperative Research and Development Award). All other authors have reported that they have no relationships relevant to the contents of this paper to disclose.

used in 69% of scans (18). Aminophylline 100 to 150 mg was administered post-stress to mitigate residual vasodilator effects during rest imaging.

Subsequently, steady-state free precession cine images were acquired to assess left ventricular function. Thirty minutes after stress, rest perfusion imaging was performed, repeating the dual-bolus method as described. A final dose of 0.05 mmol/kg gadolinium was injected after the rest perfusion study in preparation for LGE imaging. Ten minutes after rest perfusion, LGE images were obtained with a phase-sensitive inversion recovery fast gradient echo sequence.

Image analysis. CMR exams were analyzed blinded to clinical history and cardiac catheterization results by a consensus of 2 readers. Qualitative interpretation of exams was performed by a standard clinical protocol using all imaging including cine, stress/rest perfusion, and LGE. Additionally, the published Duke algorithm was applied in which LGE was used as an initial screen for obstructive CAD and stress/rest perfusion images were considered at secondary and tertiary levels of importance (19).

For fully quantitative and semiquantitative analyses, 3 stress perfusion slices per patient were divided into 12 radial segments per slice and evaluated as endocardial, epicardial, and transmural regions. Endocardial and epicardial contours were drawn manually, automatically propagated, and manually corrected when necessary, which required approximately 5 to 10 min per slice. Division into endocardial and epicardial regions was entirely computer-derived. Absolute myocardial perfusion was quantified using Fermi function constrained deconvolution methods as described previously (8,16). Semiquantitative analysis of myocardial perfusion was performed as previously described (4,8,20,21). The contrast enhancement ratio (CER) method involved the following calculation: $CER = (SI_{peak} - SI_{baseline}) / SI_{baseline}$, where SI_{peak} is the mean peak signal intensity of the myocardial region and $SI_{baseline}$ is the mean baseline signal intensity of the myocardial region. The myocardial to left ventricular upslope ratio (SLP) was calculated by dividing the initial upslope of the myocardial time-intensity curve by the initial upslope of the left ventricular time-intensity curve. The upslope integral (INT) was calculated from the area under the curve (AUC) from baseline to peak enhancement using baseline-adjusted myocardial time-intensity curves.

Endocardial flow was compared with normal flow within the slice as defined by median epicardial flow. In this manner, endocardial-to-epicardial

ratios were generated for each segment. Similarly, semiquantitative endocardial values were compared with median epicardial values within the slice. Studies were classified as abnormal when at least 2 segments had endocardial-to-epicardial ratios lower than the threshold in the distribution of the stenosed vessel. In addition to endocardial-to-epicardial-ratio analysis, the diagnostic performance of absolute endocardial flow and absolute transmural flow was evaluated.

A cardiologist blinded to the CMR results performed QCA using Quantcor software (Siemens, Forchheim, Germany). All perfusion results were correlated to QCA on a per-patient basis using a threshold of 70% stenosis.

Statistical analysis. Categorical variables are expressed as numbers and percentages. Continuous variables are presented as mean \pm SD unless otherwise specified. Receiver-operating characteristic (ROC) curves for all methods were generated with MedCalc for Windows (version 12.2.1.0, MedCalc Software, Mariakerke, Belgium). Diagnostic performance was ascertained from the AUC ROC. Comparison of ROC curves was performed by the DeLong method. There was no correction for multiple comparisons of AUC curves. Optimal sensitivity and specificity were determined by the Youden index. Sensitivity and specificity between methods were compared with McNemar test. Normally distributed data was compared with the Student *t* test. The Wilcoxon and Mann-Whitney tests were applied to non-normally distributed data.

Table 1. Patient Characteristics

Age, yrs	60 \pm 11
Female	22 (33)
Hypertension	40 (60)
Hyperlipidemia	50 (75)
Diabetes	11 (16)
Smoking	28 (42)
Family history	31 (46)
Chest pain	48 (72)
Prior MI	17 (25)
Prior PCI	17 (25)
Any stenosis \geq 70% by QCA	23 (34)
3-vessel disease	2 (3)
2-vessel disease	5 (7)
1-vessel disease	16 (24)

Values are mean \pm SD or n (%).
MI = myocardial infarction; PCI = percutaneous coronary intervention;
QCA = quantitative coronary angiography.

RESULTS

Patient characteristics. Baseline characteristics summarized in Table 1 were reflective of patients routinely referred for stress imaging exams in clinical practice. The average age was 60 years (range 38 to 85 years) and 33% were women. A history of myocardial infarction was present in 25%. Remote percutaneous coronary intervention had been performed in 25%. The prevalence of obstructive CAD by QCA ($\geq 70\%$ stenosis) was 34% (23 of 67), including 2 with 3-vessel disease and 5 with 2-vessel disease.

Threshold for abnormal perfusion. The threshold for abnormal perfusion was determined by ROC (Fig. 1). The point of maximum sensitivity and specificity occurred when endocardial flow in 2 segments was $<50\%$ below normal as defined by median epicardial flow. Thus, an endocardial to epicardial ratio <0.50 identified segments with abnormal perfusion. Thresholds for semiquantitative methods were determined in a similar manner from ROC analysis. The thresholds for semiquantitative endocardial to median epicardial ratios were: CER: 0.57; SLP: 0.67; and INT: 0.58.

Diagnostic performance. Fully quantitative perfusion (QP) performed well against QCA with a sensitivity of 87% and specificity of 93%. There were 3 false negative patients by QP, all of whom

had single-vessel disease. All patients with multi-vessel disease ($n = 7$), including 1 subject with left main disease, were correctly identified as true positives by QP. There were 3 false positive subjects by QP who had stenoses of 67%, 65%, and 2-vessel disease with stenoses of 65% and 60%. No false positive patients had myocardial infarction. Invasive measures of fractional flow reserve were not available in any patients. Representative CMR images with angiographic correlation are shown in Figure 2.

The sensitivity of semiquantitative methods was 57%, 87%, and 83% for CER, SLP, and INT, respectively. QP with a sensitivity of 87% was statistically higher than CER ($p = 0.016$) but not SLP or INT. Compared with QP, qualitative methods had similar sensitivities of 87% and 83% for the Duke algorithm and clinical interpretation, respectively.

The specificity of semiquantitative methods was 91%, 68%, and 68% for CER, SLP, and INT, respectively. QP with a specificity of 91% was statistically higher than SLP and INT ($p = 0.001$ and $p = 0.001$, respectively), but not CER. Compared with QP, qualitative approaches had statistically lower specificities of 52% and 73% for the Duke algorithm and clinical interpretation methods, respectively ($p < 0.001$ and $p = 0.004$, respectively).

Diagnostic performance of QP as determined by AUC was 92%, which was statistically superior to all semiquantitative methods (Fig. 1). AUC for CER, SLP, and INT was 78%, 82%, and 75%, respectively ($p = 0.011$, $p = 0.019$, $p = 0.004$ vs. QP, respectively). AUC for QP was also statistically superior to qualitative methods (Fig. 3). The AUC for the Duke algorithm and for clinical interpretation were 70% and 78%, respectively ($p < 0.001$ and $p < 0.001$ vs. QP, respectively). Results are summarized in Table 2.

Myocardial perfusion: absolute and endocardial/epicardial ratio. Thus far, QP has represented the endocardial-to-median epicardial perfusion ratio. However, it is also important to understand the diagnostic performance of the raw endocardial and transmural perfusion values. The optimal absolute threshold for discriminating a 70% stenosis using stress endocardial perfusion was 1.98 ml/min/g, which had an AUC of 82% ($p = 0.01$ vs. QP), sensitivity of 91%, specificity of 70%, positive predictive value of 62%, and negative predictive value of 94%. The optimal absolute threshold for stress transmural perfusion was 1.58 ml/min/g, which had an AUC of 77% ($p = 0.002$ vs. QP), sensitivity of 70%, specificity of 84%, positive predictive value of 70%, and negative predictive value of 84%.

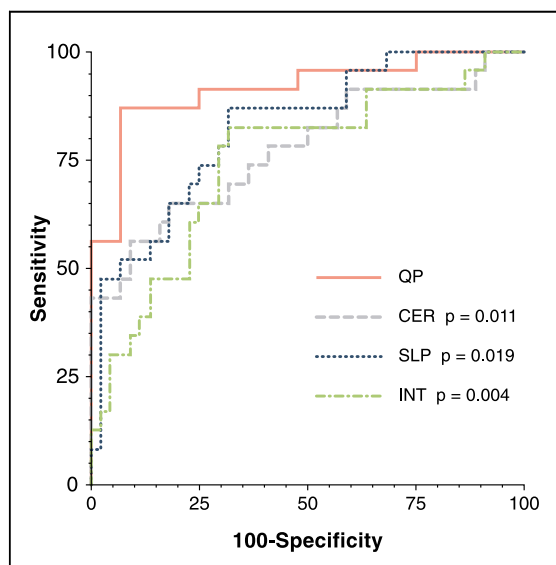
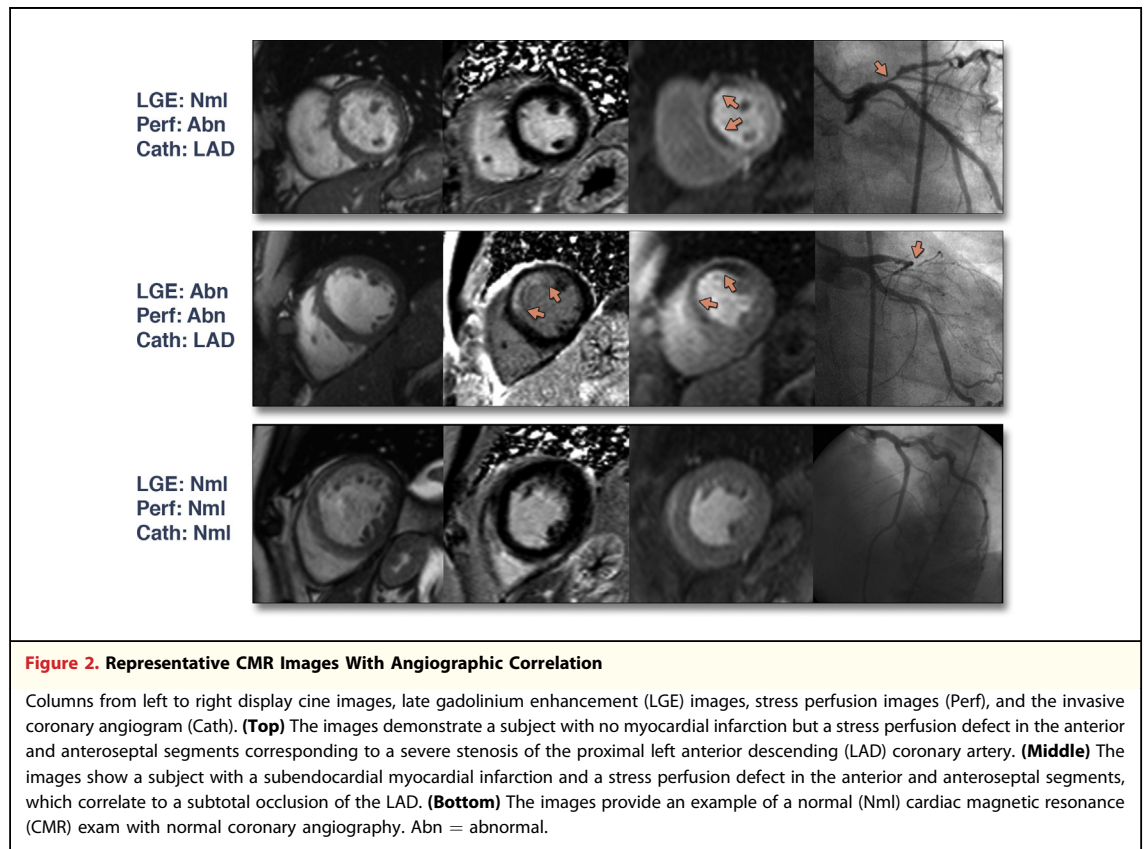


Figure 1. ROC Curves of QP and Semiquantitative Methods

The area under the curve (AUC) for fully quantitative perfusion (QP) (92) was greater than the AUC for contrast enhancement ratio (CER) (78, $p = 0.011$), myocardial to left ventricular upslope ratio (SLP) (82, $p = 0.019$), and upslope integral (INT) (75, $p = 0.004$). ROC = receiver-operating characteristic.



Absolute stress endocardial blood flow in patients with no coronary disease averaged 3.13 ± 0.61 ml/min/g, whereas endocardial blood flow in true positive perfusion defects averaged 1.20 ± 0.53 ml/min/g ($p < 0.001$). Absolute stress transmural blood flow in patients with no coronary disease averaged 2.99 ± 0.59 ml/min/g, whereas transmural blood flow in true positive perfusion defects averaged 1.73 ± 0.71 ml/min/g ($p < 0.001$). There were also significant differences between endocardial and transmural measurements among normal segments ($p = 0.015$) and ischemic segments ($p < 0.001$). The ratio of endocardial to median epicardial flow in patients with no coronary disease averaged 1.13 ± 0.19 , whereas flow ratios in true positive perfusion defects averaged 0.42 ± 0.05 ($p < 0.001$). Results are shown in [Figures 4 and 5](#).

DISCUSSION

The primary finding of this study is that a fully quantitative approach to stress perfusion CMR analysis has high diagnostic accuracy for detecting obstructive stenosis in patients with known or suspected coronary disease. Furthermore, QP outperforms

semiquantitative and qualitative interpretation methods used by experienced clinicians.

Quantitative CMR analysis could be applied in a manner similar to semiquantitative SPECT software. Semiquantitative SPECT analysis is equivalent to or minimally better than expert visual interpretation and has become an important adjunctive tool in clinical practice by offering an objective approach to differentiate normal from abnormal (22,23).

An objective approach to image analysis mitigates some of the intrinsic drawbacks of visual interpretation derived from artifact, subjective judgment, and bias. For example, discerning superimposed ischemia in the setting of myocardial infarction is a challenge in visual interpretation. However, QP performed well despite a population where a sizable portion had myocardial infarction.

QP independently has better diagnostic accuracy than qualitative methods that incorporate a combination of cine, perfusion, and LGE imaging. Simultaneous visual evaluation of stress and rest perfusion is used to identify perfusion artifacts and improve diagnostic accuracy (19). Stress perfusion and LGE imaging are commonly compared to

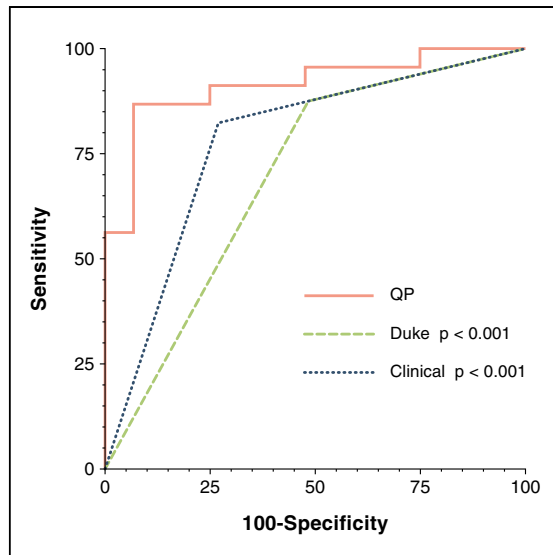


Figure 3. ROC Curves of QP and Qualitative Methods

AUC for QP (0.92) was greater than the AUC for the Duke algorithm (70, $p < 0.001$) and for clinical interpretation (78, $p < 0.001$). Abbreviations as in Figure 1.

discriminate ischemia from infarct (24). In contrast, QP utilizing stress perfusion alone performs well without the other CMR methods. Thus, stress perfusion imaging may have all the necessary information to yield a highly accurate diagnosis of flow-limiting stenosis.

With regard to other diagnostic parameters, although sensitivity was similar among methods with the exception of CER, QP specificity was significantly better than SLP, INT, and both visual methods. The improvement in specificity may help avoid unnecessary invasive testing and revascularization.

Absolute quantification of myocardial perfusion was comparable to previous data in patients with coronary disease. Transmural flow in ischemic segments averaged 1.73 ml/min/g, which is similar to the value of 1.54 ml/min/g previously reported for CMR (15). Endocardial flow in ischemic segments averaged 1.20 ml/min/g, which is similar to the value of 1.0 to 1.2 ml/min/g reported by PET for regions supplied by a >70% stenosis (25,26). No other CMR study has reported absolute endocardial flow in subjects with CAD. Our measurement of absolute endocardial flow is thus a unique aspect of this work.

In subjects without significant coronary disease, transmural myocardial blood flow averaged 2.99 ml/min/g, which was somewhat lower than the 3.39 ml/min/g reported for normal volunteers (16). However, our population likely had some degree of

endothelial dysfunction caused by early atherosclerosis, diabetes, hypertension, and dyslipidemia or nonvascular factors including left ventricular hypertrophy (27,28).

The threshold for abnormal perfusion was defined by an endocardial-to-mean epicardial ratio in this study and represented an approximately >50% reduction in flow. This threshold is consistent with previous studies (21,29–32). The endocardial-to-epicardial ratio in patients without coronary disease averaged 1.13, which is similar to the previously reported value (12).

The endocardial layer is known to be most susceptible to ischemia (33). In fact, applying endocardial rather than transmural regions of interest demonstrated higher accuracy using SLP (4). Previous studies using INT have found relative sparing of epicardial layers even in severe stenosis (21). Thus, epicardial regions are likely the best representation of preserved flow. Therefore, our analysis focused on endocardial/epicardial flow ratios as the basis of diagnosis. The median epicardial value was used as the normal reference to minimize the contribution of segments where perfusion defects become transmural. This may be why our findings differ from previous data (12). Furthermore, using an epicardial rather than remote endocardial reference may avoid problems with balanced ischemia.

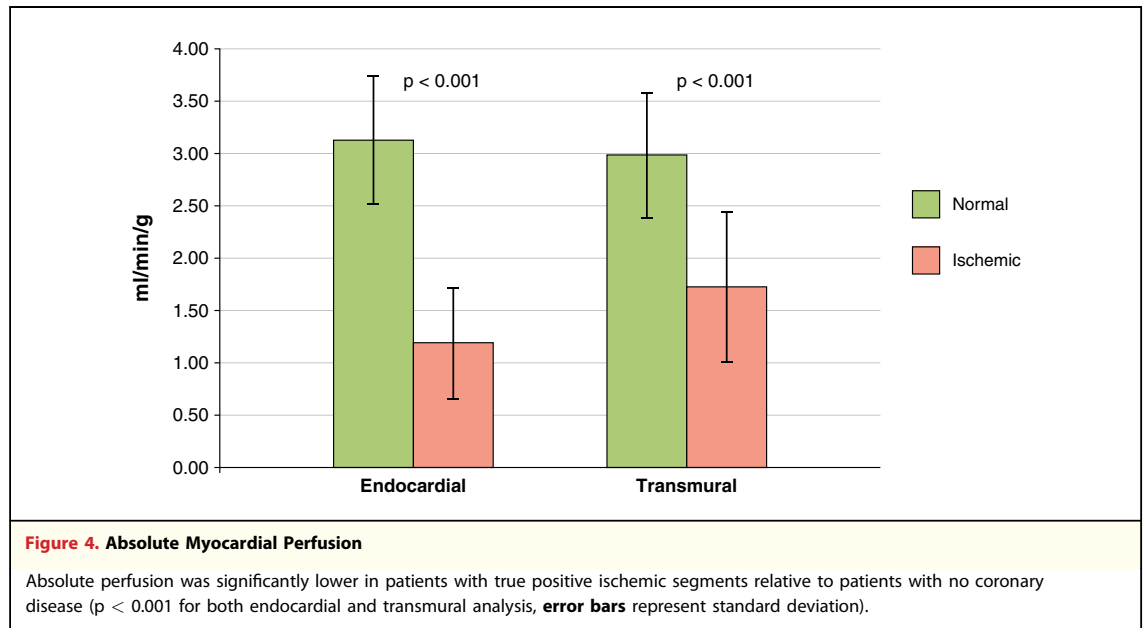
Previous studies have concluded that relative perfusion measures may represent the physiological consequences of coronary stenosis better than absolute thresholds. Models have demonstrated that absolute flow for a fixed stenosis can be variable

Table 2. Diagnostic Performance of Fully Quantitative, Semiquantitative, and Qualitative Methods To Detect a 70% Stenosis by QCA

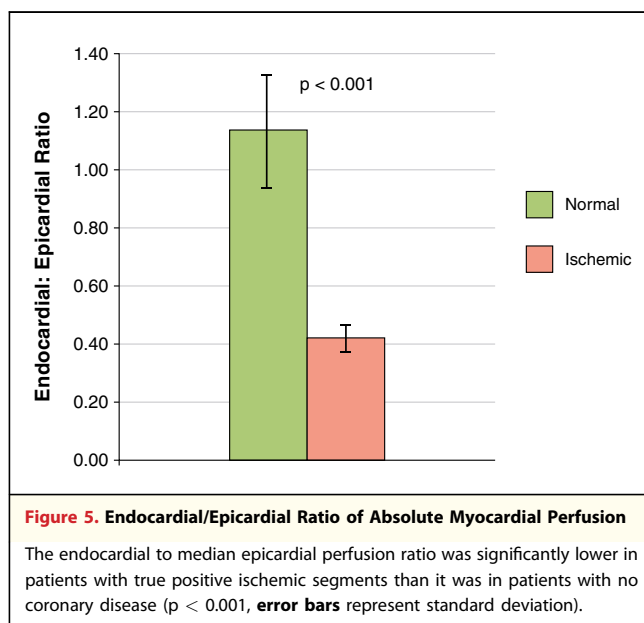
Method	AUC	Sensitivity	Specificity	PPV	NPV
QP	92 (82–97)	87 (66–97)	93 (81–99)	87 (66–97)	93 (81–99)
CER	78* (66–87)	57* (35–77)	91 (78–98)	76 (49–94)	80 (66–90)
SLP	82* (71–91)	87 (66–97)	68* (52–81)	59 (41–75)	91 (75–98)
INT	75* (63–85)	83 (61–95)	68* (52–81)	58 (39–75)	88 (72–97)
Duke	70* (57–80)	87 (66–97)	52* (37–68)	49 (33–65)	88 (70–98)
Clinical	78* (66–87)	83 (61–95)	73* (57–85)	61 (42–78)	89 (74–97)

Values are % (95% confidence intervals). * $p < 0.05$ versus QP; statistical comparison of PPV and NPV was not performed.

AUC = area under the curve; CER = contrast enhancement ratio; INT = upslope integral; NPV = negative predictive value; PPV = positive predictive value; QCA = quantitative coronary angiography; QP = fully quantitative perfusion; SLP = myocardial to left ventricular upslope ratio.



due to multiple physiologic factors and that relative flow indices more accurately reflect stenosis severity (34). Invasive fractional flow reserve relies on a relative ratio rather than an absolute value and identifies patients that benefit from revascularization (35). An absolute cutoff for normal flow by PET is difficult to define given normal subject stress values that range from 1.86 ± 0.27 to 5.05 ± 0.90 (36). Despite this limitation, PET is still effective using relative scales of flow to assess functional significance of stenosis (37,38).



This study differs from previous CMR studies in several ways. Much research has described semi-quantitative measures rather than a fully quantitative method (20,21,39–42). Although studies using SLP have reported similar accuracy in humans, the threshold value for abnormal perfusion has been difficult to define (40–42). Previous studies that used fully quantitative analysis in humans demonstrated moderate-to-high sensitivities of 78% to 93%; however, specificities were low to modest at 50% to 75% at 70% stenosis (9,12). Our improved performance could be due to multiple factors, including the use of endocardial flow, more accurate calculation of the arterial input function, signal coil intensity correction, or validated custom software (8,16). Unlike previous studies, this investigation has not excluded patients with known myocardial infarction or segments with LGE and thus is broadly applicable (11,13–15). Furthermore, this is the largest study to date involving quantification (previous studies analyzed 20 to 49 subjects) and has over twice the population previously used, comparing fully quantitative, semiquantitative, and qualitative methods of stress perfusion interpretation (10). Finally, although previous data has suggested that quantification exceeds visual interpretation, this is the first study to demonstrate statistical superiority.

Overall, the qualitative results are in the expected ranges when comparing them to large studies such as the CE-MARC (Clinical Evaluation of Magnetic Resonance Imaging in Coronary Heart

Disease) trial (3) (sensitivity/specificity = 86.5%/83.4%) and MR-IMPACT (Magnetic Resonance Imaging for Myocardial Perfusion Assessment in Coronary Artery Disease Trial) II (43) (sensitivity/specificity = 67%/61%). The sensitivities from both visual methods are moderately high at 83% to 87%, which is similar to the CE-MARC results. The specificity of clinical interpretation of 73% is somewhat lower than that reported in the CE-MARC trial but higher than in MR-IMPACT II. Of note, the high proportion of subjects with previous myocardial infarction and percutaneous coronary intervention likely contributes to the low specificity of the Duke algorithm, which is validated in patients without known CAD. This is a recognized limitation of the Duke algorithm and a potential advantage of quantification as patients with CAD commonly undergo stress testing.

Study limitations. An anatomic reference standard was used that may not reflect the flow-limiting nature of coronary stenosis. Our study had a high proportion of single-vessel disease that may have contributed to false negatives, as is also true for nuclear imaging. Parallel imaging with rate 2 temporal sensitivity encoding was incorporated during the course of the study and, though not uniformly employed, most perfusion exams (69%) used parallel imaging. Although QP could be applied in a similar

manner as semiquantitative SPECT, the use of manual contours makes this application less practical at this time, although automated contour generation is currently under development. Automated curve analysis was not used, but currently exists and would facilitate processing. Although a dual-bolus approach was used for this study, a dual-sequence approach would simplify acquisition in routine clinical practice. We did not address the prognostic value of quantitative CMR perfusion, which has been reported for PET (44).

CONCLUSIONS

Fully quantitative analysis of stress perfusion CMR has high diagnostic accuracy for detecting obstructive CAD. QP outperforms semiquantitative measures of perfusion and qualitative methods that incorporate a combination of cine, perfusion, and LGE imaging. This objective, quantitative approach has a potential adjunctive role in clinical perfusion assessment.

Reprint requests and correspondence: Dr. Andrew E. Arai, Cardiovascular and Pulmonary Branch, National Heart, Lung, and Blood Institute, National Institutes of Health, Building 10, Room B1D 416, MSC 1061, 10 Center Drive, Bethesda, Maryland 20892-1061. *E-mail:* arai@nih.gov.

REFERENCES

1. Ishida N, Sakuma H, Motoyasu M, et al. Noninfarcted myocardium: correlation between dynamic first-pass contrast-enhanced myocardial MR imaging and quantitative coronary angiography. *Radiology* 2003;229:209–16.
2. Schwitzer J, Wacker CM, van Rossum AC, et al. MR-IMPACT: comparison of perfusion-cardiac magnetic resonance with single-photon emission computed tomography for the detection of coronary artery disease in a multicentre, multivendor, randomized trial. *Eur Heart J* 2008;29:480–9.
3. Greenwood JP, Maredia N, Younger JF, et al. Cardiovascular magnetic resonance and single-photon emission computed tomography for diagnosis of coronary heart disease (CE-MARC): a prospective trial. *Lancet* 2011;379:453–60.
4. Schwitzer J, Nanz D, Kneifel S, et al. Assessment of myocardial perfusion in coronary artery disease by magnetic resonance: a comparison with positron emission tomography and coronary angiography. *Circulation* 2001;103:2230–5.
5. Axel L. Tissue mean transit time from dynamic computed tomography by a simple deconvolution technique. *Invest Radiol* 1983;18:94–9.
6. Clough AV, al-Tinawi A, Linehan JH, Dawson CA. Regional transit time estimation from image residue curves. *Ann Biomed Eng* 1994;22:128–43.
7. Jerosch-Herold M, Wilke N, Stillman AE. Magnetic resonance quantification of the myocardial perfusion reserve with a Fermi function model for constrained deconvolution. *Med Phys* 1998;25:73–84.
8. Christian TF, Rettmann DW, Aletras AH, et al. Absolute myocardial perfusion in canines measured by using dual-bolus first-pass MR imaging. *Radiology* 2004;232:677–84.
9. Costa MA, Shoemaker S, Futamatsu H, et al. Quantitative magnetic resonance perfusion imaging detects anatomic and physiologic coronary artery disease as measured by coronary angiography and fractional flow reserve. *J Am Coll Cardiol* 2007;50:514–22.
10. Futamatsu H, Wilke N, Klassen C, et al. Evaluation of cardiac magnetic resonance imaging parameters to detect anatomically and hemodynamically significant coronary artery disease. *Am Heart J* 2007;154:298–305.
11. Kurita T, Sakuma H, Onishi K, et al. Regional myocardial perfusion reserve determined using myocardial perfusion magnetic resonance imaging showed a direct correlation with coronary flow velocity reserve by Doppler flow wire. *Eur Heart J* 2009;30:444–52.
12. Patel AR, Antkowiak PF, Nandalur KR, et al. Assessment of advanced coronary artery disease: advantages of quantitative cardiac magnetic resonance perfusion analysis. *J Am Coll Cardiol* 2010;56:561–9.
13. Lockie T, Ishida M, Perera D, et al. High-resolution magnetic resonance myocardial perfusion imaging at 3.0-Tesla to detect hemodynamically significant coronary stenoses as determined by fractional flow reserve. *J Am Coll Cardiol* 2011;57:70–5.
14. Groothuis JG, Kremers FP, Beek AM, et al. Comparison of dual to single

- contrast bolus magnetic resonance myocardial perfusion imaging for detection of significant coronary artery disease. *J Magn Reson Imaging* 2010; 32:88-93.
15. Morton G, Chiribiri A, Ishida M, et al. Quantification of absolute myocardial perfusion in patients with coronary artery disease: comparison between cardiovascular magnetic resonance and positron emission tomography. *J Am Coll Cardiol* 2012;60:1546-55.
 16. Hsu LY, Rhoads KL, Holly JE, Kellman P, Aletras AH, Arai AE. Quantitative myocardial perfusion analysis with a dual-bolus contrast-enhanced first-pass MRI technique in humans. *J Magn Reson Imaging* 2006; 23:315-22.
 17. Ding S, Wolff SD, Epstein FH. Improved coverage in dynamic contrast-enhanced cardiac MRI using interleaved gradient-echo EPI. *Magn Reson Med* 1998;39:514-9.
 18. Kellman P, Epstein FH, McVeigh ER. Adaptive sensitivity encoding incorporating temporal filtering (TSENSE). *Magn Reson Med* 2001;45:846-52.
 19. Klem I, Heitner JF, Shah DJ, et al. Improved detection of coronary artery disease by stress perfusion cardiovascular magnetic resonance with the use of delayed enhancement infarction imaging. *J Am Coll Cardiol* 2006;47: 1630-8.
 20. Kraitchman DL, Wilke N, Hexeberg E, et al. Myocardial perfusion and function in dogs with moderate coronary stenosis. *Magn Reson Med* 1996;35:771-80.
 21. Klocke FJ, Simonetti OP, Judd RM, et al. Limits of detection of regional differences in vasodilated flow in viable myocardium by first-pass magnetic resonance perfusion imaging. *Circulation* 2001;104:2412-6.
 22. Slomka PJ, Nishina H, Berman DS, et al. Automated quantification of myocardial perfusion SPECT using simplified normal limits. *J Nucl Cardiol* 2005;12:66-77.
 23. Germano G, Kavanagh PB, Slomka PJ, Van Kriekinge SD, Pollard G, Berman DS. Quantitation in gated perfusion SPECT imaging: the Cedars-Sinai approach. *J Nucl Cardiol* 2007;14:433-54.
 24. Gerber BL, Raman SV, Nayak K, et al. Myocardial first-pass perfusion cardiovascular magnetic resonance: history, theory, and current state of the art. *J Cardiovasc Magn Reson* 2008;10:18.
 25. Di Carli M, Czernin J, Hoh CK, et al. Relation among stenosis severity, myocardial blood flow, and flow reserve in patients with coronary artery disease. *Circulation* 1995;91:1944-51.
 26. Muzik O, Duvernoy C, Beanlands RS, et al. Assessment of diagnostic performance of quantitative flow measurements in normal subjects and patients with angiographically documented coronary artery disease by means of nitrogen-13 ammonia and positron emission tomography. *J Am Coll Cardiol* 1998;31:534-40.
 27. Schelbert HR, Wisenberg G, Phelps ME, et al. Noninvasive assessment of coronary stenoses by myocardial imaging during pharmacologic coronary vasodilation: VI. Detection of coronary artery disease in human beings with intravenous N-13 ammonia and positron computed tomography. *Am J Cardiol* 1982;49: 1197-207.
 28. Wang L, Jerosch-Herold M, Jacobs DR Jr., Shahar E, Folsom AR. Coronary risk factors and myocardial perfusion in asymptomatic adults: the Multi-Ethnic Study of Atherosclerosis (MESA). *J Am Coll Cardiol* 2006;47: 565-72.
 29. Wilson RF, Marcus ML, White CW. Prediction of the physiologic significance of coronary arterial lesions by quantitative lesion geometry in patients with limited coronary artery disease. *Circulation* 1987;75:723-32.
 30. Gould KL, Lipscomb K. Effects of coronary stenoses on coronary flow reserve and resistance. *Am J Cardiol* 1974;34:48-55.
 31. Gould KL. Pressure-flow characteristics of coronary stenoses in unsedated dogs at rest and during coronary vasodilation. *Circ Res* 1978;43:242-53.
 32. Klocke FJ. Measurements of coronary flow reserve: defining pathophysiology versus making decisions about patient care. *Circulation* 1987;76:1183-9.
 33. Reimer KA, Lowe JE, Rasmussen MM, Jennings RB. The wavefront phenomenon of ischemic cell death: 1. Myocardial infarct size vs duration of coronary occlusion in dogs. *Circulation* 1977;56:786-94.
 34. Gould KL, Kirkeeide RL, Buchi M. Coronary flow reserve as a physiologic measure of stenosis severity. *J Am Coll Cardiol* 1990;15:459-74.
 35. De Bruyne B, Pijls NH, Kalesan B, et al., for the FAME 2 Trial Investigators. Fractional flow reserve-guided PCI versus medical therapy in stable coronary disease. *N Engl J Med* 2012;367:991-1001.
 36. Sdringola S, Johnson NP, Kirkeeide RL, Cid E, Gould KL. Impact of unexpected factors on quantitative myocardial perfusion and coronary flow reserve in young, asymptomatic volunteers. *J Am Coll Cardiol* 2011;4:402-12.
 37. Goldstein RA, Kirkeeide RL, Demer LL, et al. Relation between geometric dimensions of coronary artery stenoses and myocardial perfusion reserve in man. *J Clin Invest* 1987;79: 1473-8.
 38. Sampson UK, Dorbala S, Limaye A, Kwong R, Di Carli MF. Diagnostic accuracy of rubidium-82 myocardial perfusion imaging with hybrid positron emission tomography/computed tomography in the detection of coronary artery disease. *J Am Coll Cardiol* 2007;49:1052-8.
 39. Wilke N, Simm C, Zhang J, et al. Contrast-enhanced first pass myocardial perfusion imaging: correlation between myocardial blood flow in dogs at rest and during hyperemia. *Magn Reson Med* 1993;29:485-97.
 40. Al-Saadi N, Nagel E, Gross M, et al. Noninvasive detection of myocardial ischemia from perfusion reserve based on cardiovascular magnetic resonance. *Circulation* 2000;101:1379-83.
 41. Al-Saadi N, Nagel E, Gross M, et al. Improvement of myocardial perfusion reserve early after coronary intervention: assessment with cardiac magnetic resonance imaging. *J Am Coll Cardiol* 2000;36:1557-64.
 42. Nagel E, Klein C, Paetsch I, et al. Magnetic resonance perfusion measurements for the noninvasive detection of coronary artery disease. *Circulation* 2003;108:432-7.
 43. Schwitzer J, Wacker CM, Wilke N, et al. MR-IMPACT II: Magnetic Resonance Imaging for Myocardial Perfusion Assessment in Coronary Artery Disease Trial: perfusion-cardiac magnetic resonance vs. single-photon emission computed tomography for the detection of coronary artery disease: a comparative multicentre, multivendor trial. *Eur Heart J* 2012;34: 775-81.
 44. Herzog BA, Husmann L, Valenta I, et al. Long-term prognostic value of ¹³N-ammonia myocardial perfusion positron emission tomography added value of coronary flow reserve. *J Am Coll Cardiol* 2009;54:150-6.

Key Words: cardiac magnetic resonance ■ myocardial ischemia ■ myocardial perfusion ■ quantitative perfusion ■ stress testing.